Accurate Determination of Reactivity Ratios for Copolymerization Reactions with Reversible Propagation Mechanisms

David J. Lundberg,[1,*] Landon J. Kilgallon,[2] Julian C. Cooper,[3,4] Francesca Starvaggi,[5] Yan Xia,[5] Jeremiah A. Johnson[2,*]

Affiliations

[1]Department of Chemical Engineering, Massachusetts Institute of Technology, 77 Massachusetts Avenue, Cambridge, Massachusetts 02139, U.S.A.

[2]Department of Chemistry, Massachusetts Institute of Technology, 77 Massachusetts Avenue, Cambridge, Massachusetts 02139, U.S.A.

[3]Beckman Institute for Advanced Science and Technology, University of Illinois at Urbana-Champaign, Urbana, Illinois 61801, U.S.A.

[4]Department of Chemistry, University of Illinois at Urbana-Champaign, Urbana, Illinois 61801, U.S.A.

[5]Department of Chemistry, Stanford University, Stanford, California 94305, United States.

*Correspondence to: davidjl@mit.edu, jaj2109@mit.edu

Abstract:

An understanding of monomer sequence is required to predict and engineer the properties of copolymers. Typically, comonomer sequence is inferred or determined from reactivity ratios, which are measured through copolymerization experiments. The accurate determination of reactivity ratios from copolymerizations where one or both monomers undergo reversible propagation, however, has been complicated by difficulty in solving the underlying population balance equations, the presence of myriad copolymer equations in the literature derived under varying assumptions and simplifications, and lack of an easy to fit integrated model. Here, we rectify and assert the consistency between previously reported copolymer equations of disparate form, introduce a new method to explicitly solve the underlying population balance equations, and perform stochastic copolymerization simulations to evaluate the ability of these three methods to produce consistent comonomer consumption predictions and fits to simulated copolymerization data. We find that all methods produce consistent predictions given the same input parameters, which implies both accuracy and precision when modeling copolymerization, fitting experimental data, and making predictions of comonomer sequence. Considering this consistency, we make a recommendation to use numerical integration of the appropriate copolymer equation to fit real

copolymerization data due to its ease of implementation and single subjective parameter for implementation. We further identify the minimum number of parameters required for accurate data fitting and suggest ways to measure other information *ex situ* from copolymerization to expediate accurate fitting. Finally, the practical utility of the methods developed herein is demonstrated through fitting seven distinct copolymerization datasets which span a wide range of copolymerization reactivities.

Introduction

Copolymers are materials derived from macromolecules containing more than one type of monomer. Such materials have found widespread use in applications from injection molding manufacturing[1] to drug delivery,[2] due in part to the fine control over structure-property relationships that is enabled by simply adjusting the monomer composition at the beginning of a copolymerization reaction.[3] While this approach can provide a convenient handle to tune copolymer *composition*, the *sequence* of monomers along a copolymer backbone also strongly influences copolymer properties. For example, chemically dissimilar monomers in blocky sequences can self-assemble, whereas monomers in random or alternating sequences create polymers with properties averaged between the two monomer compositions.[4–6] In most cases, copolymer sequence cannot be strictly controlled but is instead determined stochastically on a macromolecule-by-macromolecule level based on monomer feed composition and the reactivity of each comonomer's active chain end structure with the other comonomers in solution, which is known as a *terminal* model of copolymerization. For systems containing two comonomers (monomer A and B) that undergo *irreversible* propagation reactions, this reactivity is fully described by a pair of reactivity ratios, r_A *and* r_B, which are defined as the ratio of homopropagation to cross-propagation rate coefficients:

$$r_A = k_{AA}/k_{AB}$$

$$r_B = k_{BB}/k_{BA}$$

where k_{XY} is the rate coefficient for propagation of a Y-type monomer from an X-type active chain end. Such irreversible and terminal systems have historically formed the foundation for our understanding of copolymerization. In 1944, Mayo and Lewis introduced the concept of reactivity ratios and derived the first copolymer equation, which describes the instantaneous rate of monomer consumption during a copolymerization reaction:

$$\frac{d[M_A]}{d[M_B]} = \frac{[M_A](r_A[M_A] + [M_B])}{[M_B]([M_A] + r_B[M_B])} \quad (1)$$

where $[M_A]$ and $[M_B]$ are the solution concentrations of each monomer type.[7] Equation 1, frequently referred to as the Mayo-Lewis equation, is oftentimes expressed in terms of mole fraction of each monomer in the feed solution and in the polymer. At the time of its derivation, the

differential nature of the Mayo-Lewis equation prompted the development of simple, linearized methods to extract reactivity ratios from copolymerization data generated from multiple reactions run to low conversion with different comonomer feed ratios.[8–10] Due to the difficulty in evaluating differential equations without modern computational tools, these methods have been widespread in the literature over the past seventy years; however, they are fundamentally inaccurate and have since been made unnecessary by simple integrated approaches utilizing modern computational tools. [11–15] That is, data for comonomer consumption over the course of a *single* copolymerization reaction can be fit to extract reactivity ratios simply and accurately through numerical integration of the Mayo-Lewis equation. Moreover, a simple, closed-form integrated solution of the Mayo-Lewis equation was derived by Meyer and Lowry in 1965:[16]

$$conv. = 1 - \left(\frac{f_A}{f_A^0}\right)^{r_B/(1-r_B)} \left(\frac{1-f_A}{1-f_A^0}\right)^{r_A/(1-r_A)} \left(\frac{f_A(2-r_A-r_B)+r_B-1}{f_A^0(2-r_A-r_B)+r_B-1}\right)^{r_A r_B/[(1-r_A)(1-r_B)]} \quad (2)$$

where the total monomer conversion is related to the instantaneous, f_A or f_B, and initial, f_A^0 or f_B^0, mole fractions of monomer type A or B in solution, respectively. Using Equation 2, a practitioner can conduct a *single* copolymerization reaction, periodically monitor monomer consumptions to generate multiple f_A and f_B versus conversion data points, and fit those data to extract accurate reactivity ratio values. We note that in some scenarios, Equation 2 produces numerical instabilities (e.g., when either reactivity ratio is equal to 1, or the copolymerization is occurring at the azeotropic point); however, these cases can be treated with modified equations present in an appendix of Meyer and Lowry's original publication or by studying additional initial monomer fractions. Knowledge of reactivity ratios and copolymer composition measured in this way can be used to infer comonomer sequence through heuristics or otherwise be used as inputs to stochastic copolymerization simulations to generate ensemble comonomer sequence knowledge about a specific polymer sample.[3,17] For example, blocky comonomer sequences result when both r_A and r_B are >1, or alternating comonomer sequences result when both r_A and r_B are <1.

While our understanding of irreversible copolymerization is robust and the existence of simple and validated tools for the extraction of reactivity ratios allows for rapid and accurate characterization of experimental data, such methods become inapplicable when one or both comonomers exhibit reversible propagation reactions, otherwise known as equilibrium

polymerization. Equilibrium polymerization is understood through the lens of the *thermodynamics* of a homopolymerization reaction, i.e., a monomer homopolymerizes when such homopolymerization is thermodynamically favorable. The concentration at which polymerization becomes energetically neutral is known as the equilibrium concentration, $[M]_{eq}$, which is defined at a given temperature, T, to be:

$$[M]_{eq} = \exp\left(\frac{\Delta H^{\circ}}{RT} - \frac{\Delta S^{\circ}}{R}\right) \tag{3}$$

where ΔH° and ΔS° are the standard state enthalpy and entropy of polymerization, respectably, and R is the ideal gas constant.[18] Polymerization reactions that are generally considered *irreversible* are typically exergonic to the extent of having negligibly low equilibrium concentrations and thus negligibly low rates of depropagation under most experimental conditions (e.g., the equilibrium concentration of styrene at 298K is 1 μM).[19] When monomers that exhibit reversible propagation are used in copolymerization, the rates of depropagation must be accounted for to accurately characterize the system (*vide infra*). The general scheme for a two-component equilibrium copolymerization where both monomer types can undergo reversible polymerization with penultimate effects on depropagation rates is shown in Scheme 1. This system is fully characterized by eight rate coefficients (k_1 to k_8).

$$\sim M_A^* + M_A \underset{k_2}{\overset{k_1}{\rightleftarrows}} \sim M_A M_A^*$$

$$\sim M_A^* + M_B \underset{k_4}{\overset{k_3}{\rightleftarrows}} \sim M_A M_B^*$$

$$\sim M_B^* + M_A \underset{k_6}{\overset{k_5}{\rightleftarrows}} \sim M_B M_A^*$$

$$\sim M_B^* + M_B \underset{k_8}{\overset{k_7}{\rightleftarrows}} \sim M_B M_B^*$$

Scheme 1. General model of penultimate equilibrium copolymerization where both monomer type 1 and 2 can undergo reversible propagation reactions. This model is characterized by eight separate rate coefficients (k_1 to k_8).

For this system, reactivity ratios are defined similarly to before as:

$$r_A = k_1/k_3 \tag{4}$$

$$r_B = k_7/k_5 \tag{5}$$

however, unlike two component irreversible copolymerization, knowledge of reactivity ratios is necessary but not sufficient to describe the entire system, as four additional rate coefficients are required. This general model shown in Scheme 1 conveniently provides a starting point to describe many other important models of copolymerization *via* simplifications. For example, in the case that only a single comonomer undergoes reversible copolymerization ($e.g., k_4$, $k_8 = 0$ if monomer type B polymerizes irreversibly), when the identity of the penultimate monomer in the chain does not affect the rate of a depropagation reaction (i.e., a *terminal* model instead of a *penultimate* model; $k_2 = k_6$ and $k_4 = k_8$), and where a single reversible monomer has an appreciable tendency to depolymerize from a homodyad (i.e., Lowry's case 1[20], $k_4, k_6, k_8 = 0$ if monomer type A polymerizes reversibly). We note that this model can be further generalized by adding penultimate and ante-penultimate effects on propagation and depropagation rates, respectively. While such effects are in some cases required to accurately model copolymerization kinetics, the large number of addition parameters are known to complicate analysis and lead to non-uniqueness in best fit values of reactivity ratios.[21–28]

The equilibrium concentration as defined in Eqn. 3 is identical to the ratios of rate coefficients for homopropagation and depropagation from a terminal dyad for each monomer type:

$$[A]_{eq} = \frac{k_2}{k_1} \tag{6}$$

$$[B]_{eq} = \frac{k_8}{k_7} \tag{7}$$

In stark contrast to two component irreversible copolymerization, the presence of reversible propagation reactions for one or both comonomers precludes the derivation of a closed form integrated expression analogous to the Meyer-Lowry equation that can be used to fit equilibrium copolymerization data and extract reactivity ratios or rate coefficients. As a result, practitioners have historically relied on linearized methods, simplified integrated methods, or they have erroneously applied the Meyer-Lowry equation to fit equilibrium copolymerization data. In 1960, Lowry derived copolymer equations for systems where only a single monomer was reversible, treating three cases with considerations for depropagation depending on the penultimate monomer identity.[20] Later, Hazell and Ivin,[29] as well as O'Driscoll and Gasparro,[30] applied this copolymer equation in a linearized fashion to characterize copolymerizations between sulfur dioxide and styrene, and methyl methacrylate and α-methylstyrene, respectively. Harrison et al. derived a copolymer equation to describe a system analogous to Lowry's first case but in a disparate final

form; they applied it to characterize the copolymerization of a cyclic allylic sulfide with styrene, vinyl acetate, methacrylate, and methyl methacrylate in a linearized fashion.[31] Cabello-Romero et al. applied numerical integrations of the copolymer equations developed by Lowry to describe $PEGMA_9$/DEAMEA copolymerization,[32] treating $PEGMA_9$ as the only reversible comonomer; however, better fits to data were observed when the system was treated as irreversible. Wittmer, in 1970, applied the same methodology as Lowry but derived a general copolymer equation treating both monomers as reversible.[33] Subsequently, simplified, or linearized versions of this equation have been applied,[34] notably by Bates and coworkers, to describe acrylate/dithiolane copolymerization.[35] In some cases, numerical instability during evaluation of Wittmer's copolymer equation has been noted.[36,37] Other general equilibrium copolymer equations are available in the literature, such as that from Izu and coworkers,[38] which relies on similar assumptions employed by Lowry and Wittmer but is derived using a statistical approach and appears in a disparate form. In 1987, Kruger et al.[39] derived an equilibrium copolymer equation following conceptually similar approaches as Lowry, Izu et al., and Wittmer, which has been used subsequently to characterize α-methylstyrene copolymerization with methyl methacrylate and butyl acrylate in a linearized fashion.[36,37,40–42] Following similar statistical arguments as Izu and coworkers, Szymański in 1986 developed a set of equations to characterize the equilibrium constants of Scheme 1 for the copolymerization between 1,3-dioxolane and 1,3-dioxepane, however this method required detailed microstructural analysis of the copolymer and was only applicable to living mechanisms where both comonomers undergo equilibrium polymerization.[43,44] In 2018, Register and coworkers derived an equilibrium copolymer equation to describe the copolymerization of cyclopentene and norbornene, which was fit to data in integrated form for both terminal and penultimate models.[45] Lynd and coworkers recently applied both integrated stochastic simulations and a simplified deterministic model to characterize glycolide/lactide copolymerization, treating glycolide propagation as irreversible.[46] Implementation of this method, however, was multi-step, relied on extracting homopropagation rate coefficients, and involved iteratively passing best fit rate coefficients back and forth between methods.

Notably, popular contemporary polymer chemistry textbooks either do not discuss,[47] or only briefly mention linearized methods derived from simplified copolymer equations,[48] in the context of characterizing equilibrium copolymerization. Moreover, some authors acknowledge the presence of reversible propagation in their experimental system yet choose to ignore the inclusion

of these effects when characterizing copolymerization reactivity, likely due to misconceptions about the accuracy and useability of preexisting methods.[49–51] Finally, despite the wide array of methods and simplifications employed in all the above cases, qualitative agreements between the models and experimental data were generally observed, further complicating choice of method, as even simplified or linearized methods can provide suitable fits to data under conditions where their key assumptions are violated (*vide infra*).

Taken together, these examples demonstrate that there is no consensus in the literature or pedagogy on how "best" to measure reactivity ratios for the general model of binary equilibrium copolymerization reactions shown in Scheme 1. That is, an analysis of the accuracy, precision, and practical utility of various methods is critically lacking. Further, key assumptions present in the derivations of closed-form copolymer equations for such systems (e.g., Lowry, Izu et al., Wittmer, and Kruger et al.) have never been rigorously checked for validity. Additionally, while general agreement between different types of methods (e.g., stochastic simulations and population balance modeling) has been observed in fitting and simulating copolymerization with a single reversible comonomer,[46,52] broad consistency has not been explored or established. Thus, we sought to investigate the use of various methods without rigorous simplifications to characterize equilibrium copolymerization reactivity, identify which of these methods, if any, are most accurate, and ultimately present a simple method to fit equilibrium copolymerization data to extract meaningful copolymerization reactivity information, including reactivity ratios. Our motivation to resolve this knowledge gap is threefold. First, polymers synthesized through mechanisms with accessible ceiling temperatures can produce circular, chemically recyclable materials,[53–56] and we envision copolymerization of two or more suitable comonomers to be an enabling tactic within such systems to access circular materials with performance advantaged properties. For example, butyrolactone can be copolymerized with caprolactone[57] or cyclic acetals[58] to modify crystallinity and mechanical properties, and myriad bio-derived methacrylate-type monomers can be copolymerized to tune glass transition temperature and tensile properties.[59–61] Second, the recent development of cleavable comonomers that polymerize under equilibrium conditions have shown great promise as additives to imbue degradability to both thermoplastics and thermosets. In the context of ring-opening metathesis polymerization (ROMP), low-strain cyclic silyl ethers and enol ethers were recently reported by our groups to copolymerize with traditional norbornene-based monomers to yield deconstructable linear, graft, and thermoset copolymers. [62–66] Similarly, cyclic

disulfides,[35,67] isocyanides,[51] and thioamides[68] have recently emerged as competent cleavable comonomers with broad classes of vinyl monomers *via* radical polymerization. In this context, the distribution of these comonomers within a polymer backbone (i.e., the comonomer sequence) dictates degradation properties; thus, accurate understanding of comonomer reactivity is vital for predicting and engineering the end-of-life properties of these materials. Finally, the emerging use of data driven research practices in combination with machine learning methods relies on large bodies of accurate and high-quality data to develop broadly useful tools for property and reactivity predictions.[69–72]

In this work, we investigate three distinct methods to characterize equilibrium copolymerization under batch conditions and extract reactivity information: (1) stochastic simulations, (2) kinetic and population balance modeling, and (3) direct numerical integration of an equilibrium copolymer equation. Stochastic simulations can incorporate arbitrary reactivity complexity with minimal practical issues, allowing us to adapt previously reported scripts and methods applied to irreversible copolymerization systems; however, the use of such methods for the characterization of copolymerization data is scarce and, to our knowledge, no rigorous comparisons to canonical methods for irreversible systems (e.g., the Meyer-Lowry equation) have been conducted. On the other hand, population balance modeling can be viewed as a kinetically accurate way to describe monomer consumption over the course of a polymerization reaction, as has been shown previously for irreversible copolymerization.[12] Unfortunately, previous attempts to model equilibrium copolymerization with population balance equations have noted an apparent need to account for every possible monomer sequence when both monomers undergo reversible polymerization, which necessitates the use of a computationally infeasible number of equations; thus, simplifications have been widely adopted.[46,73] Here, to make kinetic and population balance modeling of equilibrium copolymerization tractable, we introduce a novel technique that preserves the relative rates of monomer consumption reactions while significantly reducing the number of equations required to accurately describe the system. Finally, we reevaluate three general equilibrium copolymer equations from the literature,[33,38] rectify critical errors present in their initial reports and show that they are broadly equivalent despite their disparate forms.

Upon comparison, all three methods are shown to produce consistent predictions of equilibrium copolymerization when given the same input parameters across a vast input space of copolymerization reactivity, comonomer feed composition, and reaction rates. Correspondingly,

all three methods can accurately fit model equilibrium copolymerization data. While all three methods are consistent, we make a recommendation to use numerical integration of a copolymer equation as it is computationally most efficient and its results are not affected by additional parameters such as number of equations solved, targeted chain length, or number of chains simulated. Finally, the utility of the methods developed herein is demonstrated through the fitting of seven copolymerization reactions, including two which have previously been fit under invalid assumption of irreversibility for one or both comonomers. For these cases, use of an accurate method provides statistically significantly different measurements of rate coefficients that agree with canonical knowledge of comonomer reactivities. Altogether, this work advances the understanding of equilibrium copolymerization and establishes the accuracy and precision of easy-to-use methods to measure accurate reactivity information from equilibrium copolymerization data.

Survey of Methods

Stochastic Simulation

Stochastic simulations have been widely employed to model copolymerization and assess comonomer sequence.[17,46,74,75] These methods consider copolymerization on a macromolecule-by-macromolecule basis and determine which reaction will occur based on probabilities proportional to the values of reaction rates. At each simulation step, the probability of each reaction, p_i, is calculated as follows:

$$p_i = \frac{r_i}{\sum_n r_n} \tag{8}$$

where r_i is the rate of reaction type i (i.e., each possible reaction shown in Scheme 1). A reaction is selected and executed stochastically based on these probabilities and the system is updated at each step; a monomer reacts and is removed from the pool in a propagation event or depropagated from a chain end and added back to the monomer pool. Subsequently, the composition of a polymer chain in the simulation is modified. This process is repeated until the monomer pool is exhausted or until the polymerization reaches equilibrium (i.e., the rates of propagation and depropagation are equal). The stochastic simulation method used in this work is similar to those reported previously following a general kinetic Monte Carlo (KMC) scheme but has been modified to include the reaction steps consistent with the general model shown in Scheme 1 (see the Stochastic Simulations section of the Supporting Information for details).[17,46] For this method, we found that

typically 1,000 chains were sufficient to model copolymerization (Figure S6); we employed 5,000 to 10,000 for the comparisons shown in this work.

Kinetic and Population Balance Modeling of Equilibrium Copolymerization

Population balance modeling of copolymerization reactions relies on simultaneously integrating the set of coupled ordinary differential equations (ODEs) describing the concentrations of each species in a system.[12] Such methods have been associated with a problem of needing to account for every possible comonomer sequence in a polymer chain, as the active species 'revealed' by a depropagation reaction, as well as the identity of this 'new' chain end's penultimate unit, was believed to be required to accurately account for reaction rates, even when using a terminal model.[46,73] Thus, the number of equations to solve would scale as 2^n where n is the maximum degree of polymerization; such an approach becomes infeasible even for modest values of n. This drawback has prompted the use of simplifications, e.g., limiting the maximum degree of polymerization to relatively low values or treating only a single monomer type as reversible, to characterize or model equilibrium copolymerization reactions. We note, however, that this dilemma only manifests in the case where both comonomers can undergo equilibrium polymerization. When a single equilibrium comonomer is used, the number of differential equations describing the propagating polymer chain species required to *accurately* characterize comonomer consumption has an upper limit equal to $n + 1$.[46] Once a chain propagates an irreversible comonomer, all sequence information preceding that unit in the chain has no influence on any subsequent (de)propagation reactions and thus tracking it is not required. While methods exist to further reduce the number of equations required, as demonstrated by Hutchinson [52,76,77] and Penlidis,[78,79] these methods rely on implementing an analogous assumption as that of Lowry, Izu, Witter, and Kruger in their copolymer equation derivations (*vide infra*).

Here, we present a resolution to the apparent dilemma when both comonomers undergo equilibrium polymerization by keeping track of comonomer sequence information *implicitly* at each position in the chain as a probability mass function describing the eight possible dyads. In this way, the identity of the antepenultimate chain unit revealed by a depolymerization reaction of the n^{th} chain position is accounted for stochastically based on the population of dyads ending at the $(n-1)^{\text{th}}$ position. This treatment relies on the assumption that the rates of depropagation reactions from each possible terminal dyad do not depend on the identity of the antepenultimate

monomer, which is true under the penultimate model of equilibrium copolymerization (Scheme 1). Compared to explicitly tracking all monomer sequences, this approach requires significantly fewer equations (approximately $8n$ versus 2^n), does not require any assumptions regarding previous sequence information, yet maintains accurate predictions of comonomer consumption rates (see the Population Balance Kinetic Modeling Section of the Supporting Information for details).

Equilibrium Copolymer Equation

Multiple copolymer equations that describe either the general equilibrium copolymerization model present in Scheme 1 or various simplifications of it have been reported in the literature over the past sixty years. Here, we focus on those that have been presented for the general model of Scheme 1 as they can be easily modified to describe more simplified systems with no loss in generality. Wittmer,[33] Izu et al.,[38] and Kruger et al.[39] have presented copolymer equations that describe the general equilibrium copolymerization model shown in Scheme 1; however, we have found critical errors in the equations derived by Wittmer and Izu et al. and present rectified forms of their equations here (see the Equilibrium Copolymer Equations Section of the Supporting Information for details). These errors likely explain previous observations of instability during evaluation of the Wittmer equations.[36,37] Although these three copolymer equations are derived using different approaches and appear in disparate forms, we find that they are consistent with each other and provide practically indistinguishable results when evaluated with the same parameters (Figures S2-S5). Considering this agreement, for this work we choose to present in the main text and use for evaluation only the model as derived by Izu and coworkers due to its more intuitive parameter assignment and simpler form, which appears as a traditional copolymer equation differential for relative monomer consumption (Eqn. 10) in addition to four coupled algebraic equations (Eqns. 11-14):

$$\frac{d[A]}{d[B]} = -\frac{ak_1[A] + bk_5[A] - a[(1-\epsilon)k_6 + \epsilon k_2]}{bk_7[B] + ak_3[B] - b[(1-\eta)k_4 + \eta k_8]} \tag{10}$$

$$a + b = 1 \tag{11}$$

$$a[k_3[B] + (1-\epsilon)k_6] = b[k_5[A] + (1-\eta)k_4] \tag{12}$$

$$b\epsilon(1-\eta)k_4 = a[\epsilon(k_1[A] + k_2 + k_3[B]) - (k_1[A] + \epsilon^2 k_2)] \tag{13}$$

$$b\epsilon(1-\eta)k_4 = a[\epsilon(k_1[A] + k_2 + k_3[B]) - (k_1[A] + \epsilon^2 k_2)] \quad (14)$$

Where rate coefficients, k_i's, are defined analogously to Scheme 1, a and b are the fraction of chain ends containing active monomer types A and B, respectively, and ϵ and η are the fraction of chains with A or B active units that exist as terminal AA or BB homodyads, respectively. Knowledge of penultimate monomer identities encapsulated in the parameters ϵ and η are required to calculate the rates of all possible (de)propagation reactions, which necessitates the form of the copolymer equation (one differential equation and multiple coupled algebraic equations). We note that the copolymer equations derived by Wittmer and Krueger et al. are also presented as a combination of a single differential equation and multiple coupled algebraic equations (see Eqns. S10-12 and Eqns. S31, S38-S43). Direct numerical integration of Eqn. 10, while simultaneously solving Eqn. 11-14 at each timestep, can generate predictions of monomer consumption during equilibrium copolymerization reactions. Practically, it is more convenient to integrate a mole fraction form of Eqn. 10 due to the ease of comparison with experimental measurements of monomer conversions:

$$\frac{df_A}{dX} = \frac{f_A - F_A}{1-X} \quad (15)$$

$$F_A = \frac{ak_1[A] + bk_5[A] - a[(1-\epsilon)k_6 + \epsilon k_2]}{ak_1[A] + bk_5[A] - a[(1-\epsilon)k_6 + \epsilon k_2] + bk_7[B] + ak_3[B] - b[(1-\eta)k_4 + \eta k_8]} \quad (16)$$

where f_A and F_A are the mole fraction of monomer A in the feed and instantaneous incorporation fraction of monomer A into the polymer, respectively. We note a foundational assumption in the derivation of the closed-form copolymer equations considering reversible propagation (e.g., Izu, Wittmer, Krueger, and Lowry). In all cases, the concentrations of all terminal run lengths for reversible comonomer(s) of the same type are treated as geometrically proportional with the ratio α:

$$\frac{[\sim M_B M_A M_A^*]}{[\sim M_B M_A^*]} = \frac{[\sim M_B M_A M_A M_A^*]}{[\sim M_B M_A M_A^*]} = \cdots = \frac{[\sim M_B (M_A)_{n+1} M_A^*]}{[\sim M_B (M_A)_n M_A^*]} = \alpha < 1 \quad (17)$$

where $\alpha < 1$. Practically, this implies that the steady state distribution of reversible comonomer run lengths exists from time zero. The validity of this assumption will be discussed below but is found to be generally satisfied for modest chain lengths.

Method Comparison

Having proposed a new method for population balance modeling of equilibrium copolymerization, rectified the available copolymer equations presented in the literature, and with stochastic

simulation scripts in hand, we set out to compare the precision of these three methods given the same input parameters. Because the results of these methods can be sensitive to user-defined parameters (e.g., number of macromolecule chains simulated, integration time-step size, and number of equations to track) an initial optimization was performed to identify suitable conditions for all models to ensure accuracy across a sub-set of input parameters (see the Method Comparison Details Section of the Supporting Information). In line with widely used methods to characterize irreversible copolymerization, for our method comparison we considered a system with fast initiation relative to propagation, no termination or chain transfer, and a targeted degree of polymerization of 1,000. A representative plot of copolymerization data after this initial optimization is shown in Figure 1A, which suggests excellent agreement between the three methods. For all cases presented herein, agreement in comonomer consumption predictions as shown in Figure 1A is accompanied by agreement in predicted rates of reactions (Figure 1B). While stochastic simulation methods predict reaction rates that can vary with a visible amount of simulation noise, in general we observe that this noise has a negligible effect on predicted copolymerization data. Increasing the size of stochastic simulations could reduce noise at a cost of increased computational load but with no increase in precision between methods (Figures S4 and S5). To further assess the agreement between methods, we simulated 200 randomly generated sets of input parameters with all three methods and calculated the sum of square residuals at 100 points across the simulated conversion range. Between the three methods, three possible sum of squared residual (SSR) values were calculated, and the largest value is reported in Figure 1C, sorted by the type of copolymerization behavior as determined by reactivity ratios heuristics (all values are listed in Table S1). Over all conditions and copolymerization behaviors, the precision of these methods is excellent, producing SSR values $< 10^{-3}$, representative of at most a 0.32% deviation in monomer conversion predictions at all points. For comparison, 1% deviation between values, which is often less than experimental uncertainty, would give an SSR value of 10^{-2}. Notably, these SSR values are significantly lower than those obtained from fitting experimental data sets, supporting the claim that such discrepancies do not affect the ability of one or all methods to fit real experimental data (*vide infra*).

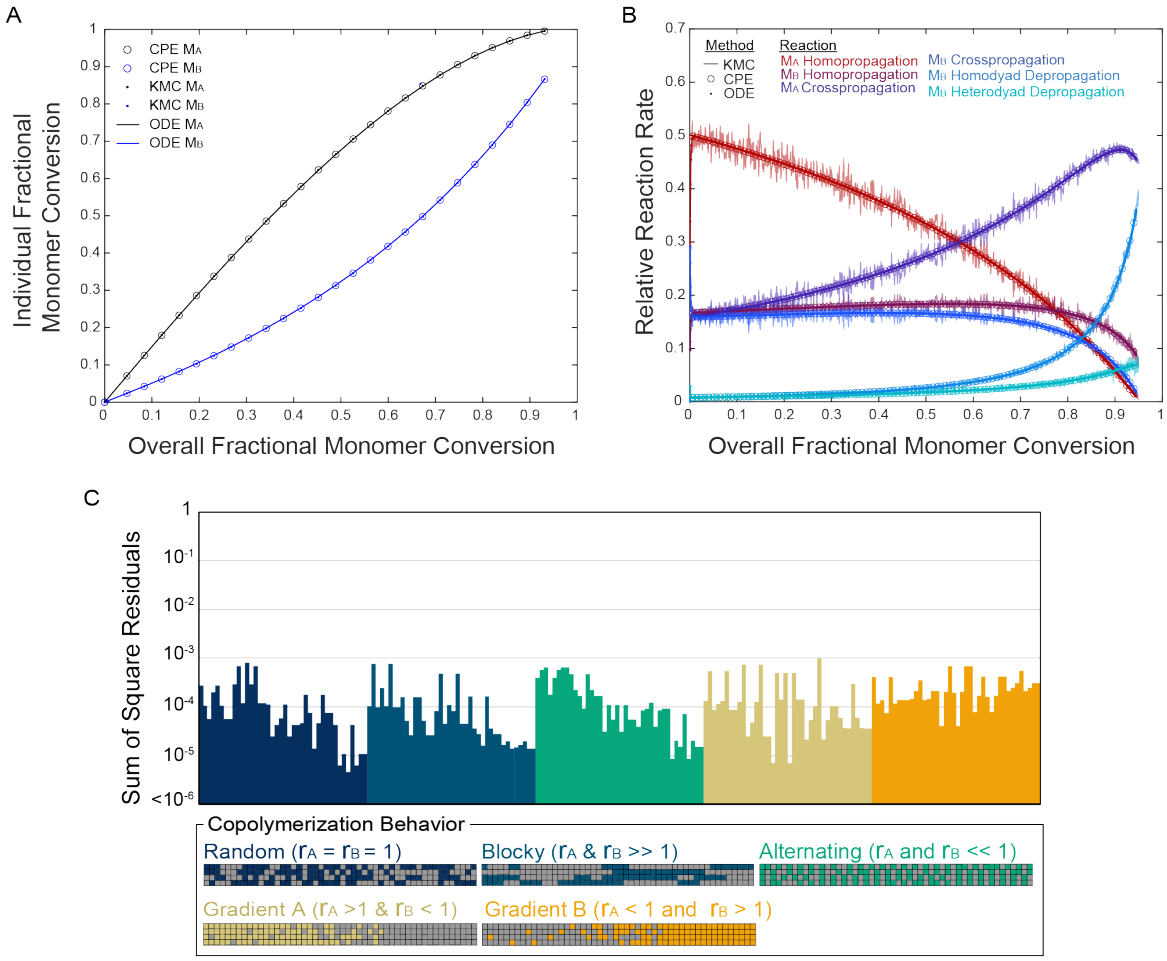

Figure 1. A. Method comparison demonstrating the consistent monomer conversion data from each of the three models (stochastic simulations 'KMC', copolymer equation integration 'CPE', population balance modeling 'ODE') for the same set of input parameters ($f_{M_A,0} = 0.5, r_A = 5, r_B = 1, k_6 = k_8 = 0.1, [M]_0 = 1M$). **B.** Calculated relative reaction rates over the course of the polymerization described in panel A showing the agreement between the three methods. Consistency between monomer conversion data and relative reaction rates was observed in all cases explored. **C.** The maximum sum of square residuals (SSR) between the three models when comparing across various copolymerization behaviors, denoted by color. SSR values were found to be less than 10^{-3} (corresponding to an R^2 value of >0.999), which is an order of magnitude lower than the value obtained with a 1% difference in prediction at each of the 100 data points. These data confirm that all models are precise and accurate over the reactivity space explored.

In specific cases, there are small deviations between these methods that can be attributed to the steady state assumption implicit in the derivation of the copolymer equation. As mentioned above, this assumption implies that the entire distribution of monomer run lengths already exists at time zero. In other words, depropagation reactions can occur immediately. For polymers that ultimately reach an appreciable length (degrees of polymerization >~100), such an assumption causes only

small deviation, as shown in Figure 1C; however, for short chains where polymerization is initiated under conditions that strongly favor depropagation reactions, discrepancies can result between copolymer equation integration and stochastic simulations / population balance methods (see the Supporting Information for complete discussion). In practice, such conditions achieve low levels of monomer conversion and can be identified and avoided *a priori* to data fitting based on knowledge of monomer to initiator ratio and initial monomer concentration.

While these results confirm the *precision* of the three methods in describing equilibrium copolymerization reactions, the *accuracy* of these methods to faithfully reproduce true equilibrium copolymerization behavior warrants further discussion. Previously, the accuracy of various methods to fit *irreversible* copolymerization models has been assessed by comparing predictions of copolymerization kinetic data between numerical integration of the population balance equations against the Meyer-Lowry equation or integration of the Mayo-Lewis equation. In this way, population balance methods have been viewed as a set of *true* data to serve as a baseline for comparison. As mentioned previously, to-date, no general population balance modeling for equilibrium copolymerization has been rigorously explored. Because we have shown that our modified population balance method maintains the consumption rates of monomers, this method will produce copolymerization predictions identical to an exhaustive population balance method. Considering this, we propose that the three methods explored herein do *accurately* describe equilibrium copolymerization reactions. Further, agreement of all methods with stochastic simulations implies that regardless of which method is used to characterize a copolymerization system and extract rate parameters, any subsequent predictions of comonomer sequence using stochastic simulations will produce self-consistent results. Altogether, we have established the *accuracy* and *precision* of stochastic simulations, population balance modeling, and numerical integration of a copolymer equation to simulate equilibrium copolymerization reactions.

Data Fitting Ability

We next sought to assess the practicality and accuracy of these methods to *fit* model generated copolymerization data and return predictions of kinetic parameters. Here we note that despite the accuracy and precision of the three methods investigated, numerical integration of a suitable copolymer equation consistently proved to be the most computationally efficient and relies only on a single user-defined parameter (the integration timestep) and thus was used for all further

data fitting. Model copolymerization data were generated spanning a wide range of input parameters and subsequently these datasets were fit using a non-linear least squares method (see the Fitting Model Data section of the Supporting Information). Initially, we explored the ability of this method to fit accurate kinetic parameters for a system with varying feed ratios of monomers. For this example, we simulated a system with a single reversible monomer (M_B) and fit four parameters: k_8, k_4, r_A, and r_B. The simulated data and best fit lines for this case are shown in Figure 2A, illustrating excellent qualitative agreement. Concomitantly, the best fit values of these parameters accurately match those used to generate the simulated data across all initial monomer concentrations (Figure 2B). Further, analogous fitting of data for systems at a fixed commoner ratio but with varying initial concentrations produced accurate rate coefficient fits (Figures 2C and 2D). Similar analyses were conducted for systems containing two equilibrium comonomers, systems with only terminal effects, or combinations thereof; in all cases, accurate kinetic parameters were reproduced efficiently with this fitting routine.

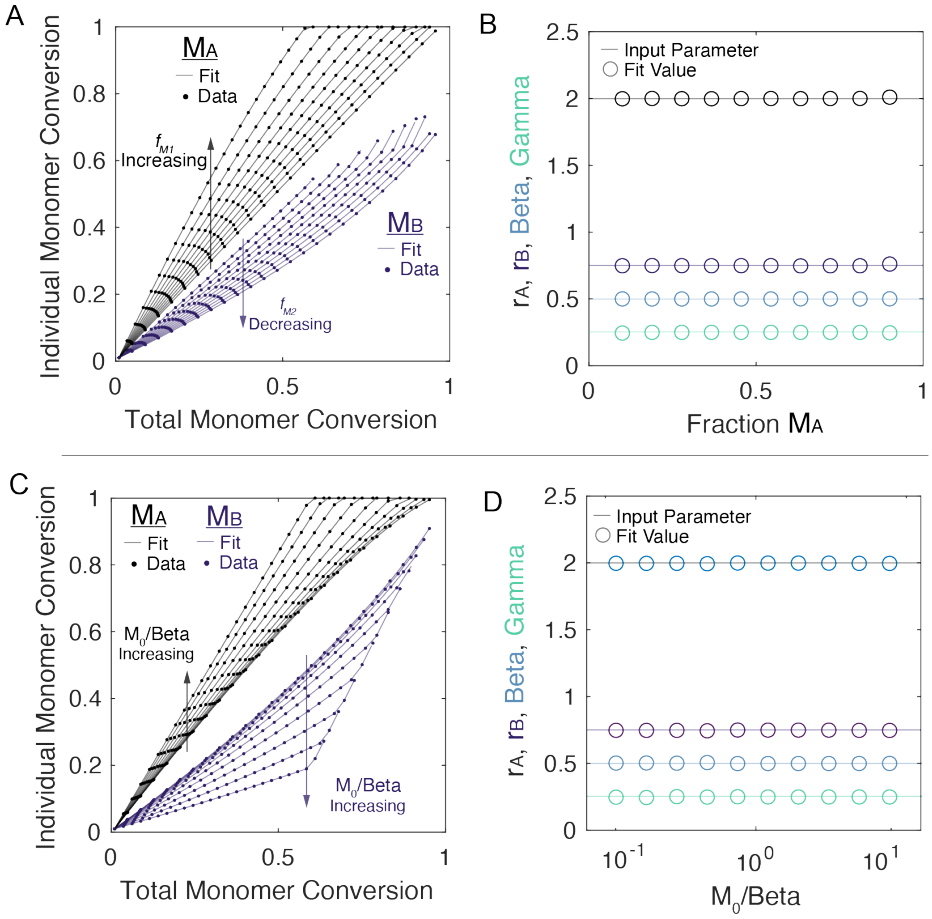

Figure 2. Results of fitting model data generated with known reactivity parameters using integration of a copolymer equation. **A.** Model data and lines of best fit for constant reactivity parameters with varying initial monomer fractions. **B.** Reactivity parameter estimations from the data fit in panel A. The fitting procedures accurately estimates the known parameters used to generate the model data set across all initial monomer fractions. **C.** Model data and lines of best fit for constant reactivity parameters with varying polymerization concentrations. **D.** Reactivity parameter estimations from data fit in Panel C. The fitting procedures accurately estimates the known parameters used to generate the model data set across all polymerization concentrations. Uncertainty in fit parameters is smaller than the marker size.

A critical point worth justification and further discussion is the lumping of multiple rate coefficients into reactivity ratios to reduce the number of fit parameters required (e.g., $r_A = k_1/k_3$ and $r_B = k_7/k_5$). In practice, this simplification can be done by setting the values of k_1 and k_7 equal to 1 and equating r_A to $1/k_3$ and r_B to $1/k_5$, which reduces the number of fit parameters by two. A beneficial consequence of this simplification is that values of equilibrium monomer concentrations, which can be measured *a priori*, are then equal to the homo-depropagation rate coefficients:

$$[A]_{eq} = \frac{k_2}{k_1} = \frac{k_2}{1} = k_2$$

$$[B]_{eq} = \frac{k_8}{k_7} = \frac{k_8}{1} = k_8$$

Such a simplification allows input of previously measured equilibrium monomer concentrations when fitting data, which can improve the precision of the fitting by reducing the number of fit parameters or serve as a check for feasibility by comparison against the best fit value obtained. The major assumption of this simplification is that the *true* magnitude of these rate coefficients is inconsequential for modeling copolymerization data in the comonomer consumption form. Such an assumption is valid in the case of two component irreversible copolymerization, as can be seen by inspection of the Mayo-Lewis equation wherein all rate coefficients appear in terms solely of reactivity ratios, and in some simplified forms of Scheme 1 as described by Lowry.[7,20] Conversely, Equation 10 (and the copolymer equations from Wittmer and Krueger et al., Eqns. S19-S21 and Eqns. S31, S38-43, respectively), as well as Eqns. 11–14, are not in such a form, suggesting that the magnitude of individual rate coefficients may affect copolymerization calculations. To test the validity of this assumption for the equations used, we calculated the values of parameters a, b, ϵ, and η for the set of rate coefficients used to generate Figure 1A but with varying values of the ratio

k_1/k_7 with k_1 held at a value of 1. Under these conditions the values of a and b, but not ϵ or η, varied with the value of k_1/k_7 (Figure S17A). Accordingly, the calculated rates for each possible reaction during a copolymerization simulation were significantly different between simulations when run with k_1/k_7 values of 0.1 and 10 (Figure S17B). Surprisingly, despite these differing values in reaction rates, indistinguishable predictions of comonomer consumption were produced between the two simulations and myriad others performed with significantly varying monomer compositions and rate parameters. The observed consistency across predictions of comonomer consumption confirms that the true magnitudes of homopropagation rate coefficients are inconsequential for fitting experimental data in the comonomer consumption form and justify the simplification of fixing both homopropagation rate coefficients to 1 during data fitting. Further, this simplification does not affect predictions of comonomer sequence determined through stochastic simulations (Figure S18). Overall, the eight total rate coefficients in Scheme 1 can be lumped into 6 fit parameters (r_a, r_b, k_2, k_4, k_6, k_8), two of which (k_2 and k_6) can then be treated as equal to equilibrium monomer concentrations, which can be routinely measured with high precision independently from copolymerization experiments.[80–82] To explicitly distinguish when best fit values for rate coefficients are obtained under this assumption, we adopt the following nomenclature for the remainder of this manuscript:

$$[A]_{eq} = k_2 = \beta_A$$

$$[B]_{eq} = k_8 = \beta_B$$

$$k_6 = \gamma_A$$

$$k_4 = \gamma_B$$

Systematic Inaccuracy of Previously Reported Linearized and Simplified Methods

Historically, linearized methods have been pervasive in the measurement of reactivity ratios for irreversible copolymerization reactions. That is, the differential form of the Mayo-Lewis equation was re-interpreted into various forms to fit reactivity ratios using measurements of monomer conversion from reactions with different initial monomer composition run to vanishingly low conversion.[8,9] The crux of these methods is the assumption that at low conversion, the feed concentrations of monomer remain relatively constant. As stated previously, these linearized methods have been shown to be systematically inaccurate in the case of irreversible polymerization reactions.[12] Motivated by the wide application of linearized methods to describe copolymerization

reactions with reversible propagation mechanisms in the literature,[29,30,34,35] we sought to analyze the general accuracy of such methods. To do so, model copolymerization data were generated with known reactivity parameters and were fit to a linearized form of Eqn. 10 (see the Linearized Methods section of the Supporting Information). The results of this linearized fitting for a test case run to varyingly low values of monomer conversion are shown in Figure 3A. Across all conversion values, inaccurate parameter values are obtained from the best fits. Additionally, we fit model data at constant low conversion (5%) with varying initial monomer fractions and found that accurate values of only some parameters are returned at specific initial monomer compositions; however, no composition will return accurate values for all parameters (Figure 3B), further verifying the inaccuracy of linearized methods. For this parameter set and all others explored (Figures S14-S20), the best fit value of every parameter is systematically inaccurate compared to the true value regardless of the total monomer conversion value or monomer loading. These results indicate that linearized methods to measure kinetic parameters for copolymerization reactions with reversible propagation methods are systematically inaccurate and we discourage their further use.

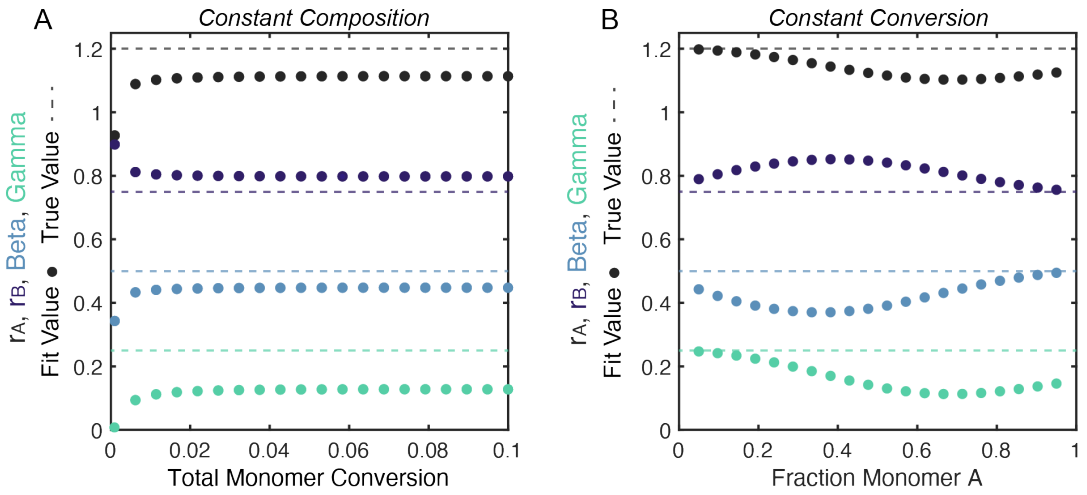

Figure 3. Evaluation of simulated data fitting using a linearization of Equation 10. **A.** Data fitting for 30 mol% monomer A at a 1M initial concentration for various total monomer conversion values. Systematic errors are observed for all parameters at all conversion values, indicating the inaccuracy of linearization methods even at low total monomer conversion values. **B.** Data fitting for varying initial monomer fractions at a 1M initial concentration stopping at 5% total monomer conversion. Accurate values of only some parameters are returned at specific initial monomer compositions, however no composition will return accurate values for all parameters, verifying the inaccuracy of linearization methods.

Application of Method to Fit Equilibrium Copolymerization Data

Given the accuracy and precision of copolymer equation integration to describe equilibrium copolymerization reactions and fit rate coefficients, we sought to apply this method to the characterization of real experimental data. Initially, we explored low-strain cyclic olefins containing endocyclic cleavable moieties, which our groups have applied in the context of degradable and recyclable thermoplastics and thermosets.[62–64,83] For these applications, knowledge of comonomer sequence is vital for predicting the molecular weights and functionalities of the fragments obtained after cleavable bond scission.[84] Previously, we reported the copolymerization between an eight-membered cyclic bifunctional silyl ether (**iPrSi-8**) with an *endo*-norbornene imide (***endo*-NB**) and measured a pair of reactivity ratios for this system using a linearized Mayo-Lewis method.[62] Subsequently, we reported the equilibrium copolymerization behavior of **iPrSi-8**,[63] which, combined with the findings above, would suggest that our previous copolymerization analysis was erroneous. Here, to reevaluate this system, we acquired an integrated copolymerization data set using real-time ^{1}H NMR spectroscopy, which allowed for facile calculation of comonomer conversion values over the course of the entire copolymerization reaction (see the Characterization of Experimental Data Section of the Supporting Information).

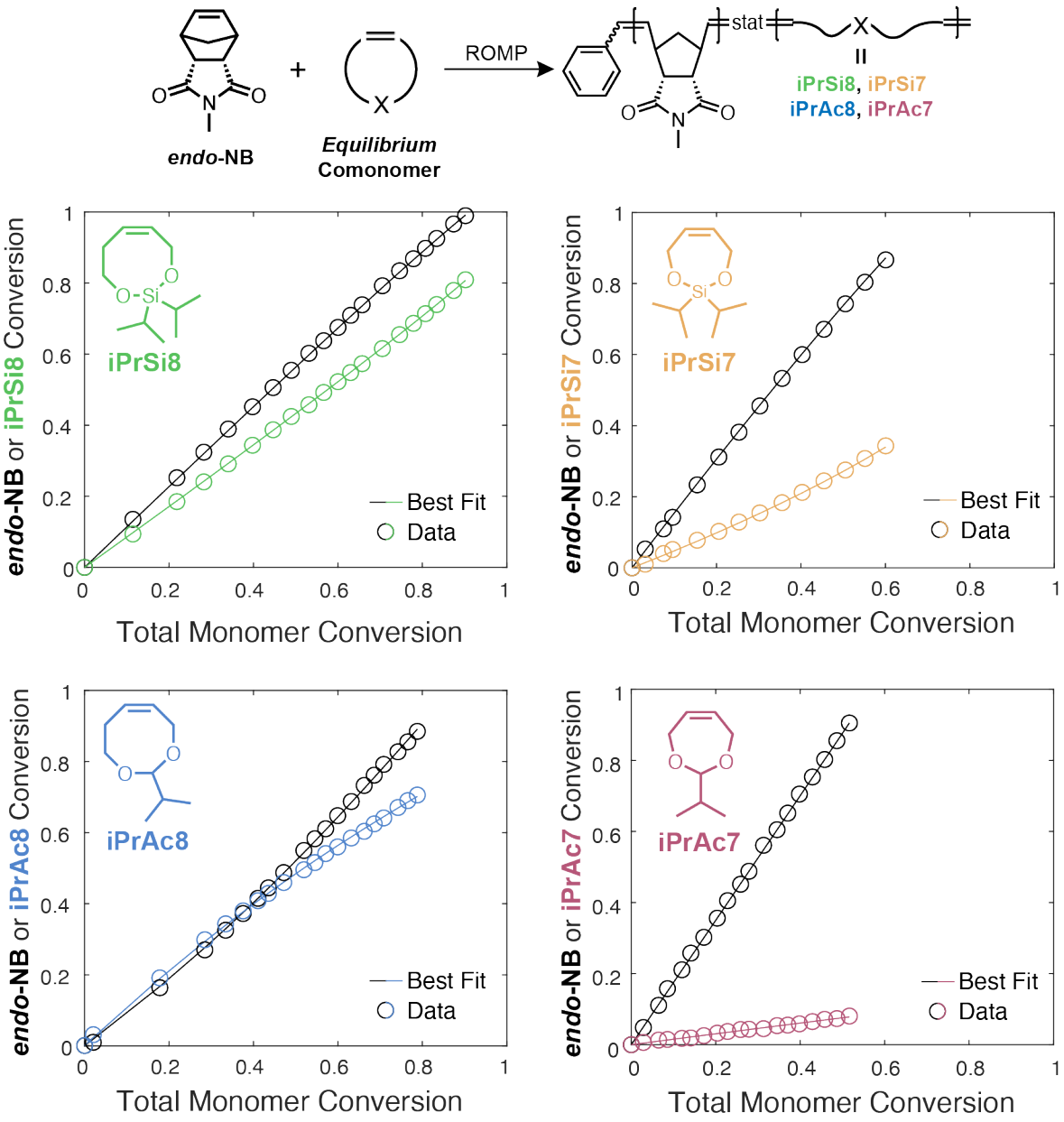

Figure 4. Fitting of equilibrium copolymerization data between *endo*-NB and a library of low-strain cyclic olefins containing endo-cyclic cleavable moieties. The copolymerization was conducted at room temperature in chloroform with an initial monomer concentration of 200 mM and a 1:1 *endo*-NB to comonomer ratio, with a 200:1 monomer to catalyst ratio. The fitted parameters are listed in Table 1. For all cases, fitting to the generalized equilibrium copolymerization model gives excellent agreement with data.

These data are shown in Figure 3B for an equimolar monomer ratio with an initial monomer concentration of 200 mM in dichloromethane using Grubbs third generation bis-pyridyl complex as the initiator. Visually, the model fits the data well and captures the halting of the reaction at

near quantitative ***endo*-NB** conversion without complete **iPrSi8** consumption, which is a hallmark of equilibrium (co)polymerization. The best-fit parameters for this system are listed in Table 1 (with values of uncertainty determined through bootstrapping methods, see Supporting Information section Uncertainty Analysis for full details), and the obtained reactivity ratio values ($r_{\textbf{endo-NB}}$ = 0.4 and $r_{\textbf{iPrSi8}}$ = 0.08) are statistically significantly different than those we reported previously[62] (i.e., $r_{\textbf{endo-NB}}$ = 0.61 and $r_{\textbf{iPrSi8}}$ = 0.72). We note that the fit value of γ for this monomer pair is statistically significantly different than the equilibrium concentration measured for **iPrSi8**. This difference is consistent with previous reports on ring-closing metathesis where reaction rates are affected by exocyclic allylic substituent bulk,[85] and supports the inclusion of penultimate effects in characterizing this reaction. Moreover, these corrected values correspond to more strongly alternating copolymerization behavior based on traditional heuristics (i.e., the value of $r_{endoNb} \times r_{iPrSi8}$ is lower), which is illustrated by stochastic simulations of comonomer sequences (Figure S34). Encouraged by this result, we characterized polymerizations of three other equilibrium comonomers of interest (**iPrSi7, iPrAc7,** and **iPrAc8** in Figure 3) with ***endo*-NB**. Our groups have previously employed these comonomers (alongside **iPrSi-8**) as additives to enable degradable poly(*endo*-dicyclopentadiene) thermoset materials, an application where prediction of network degradability is highly sensitive to comonomer reactivity, and for which ***endo*-NB** serves here as a surrogate to assess the reactivity in these systems without the possibility of cross-linking.[83] Similar real-time experiments were performed and comonomer consumption data for **iPrSi7**, **iPrAc7**, and **iPrSi8** were fit analogously. We note than **iPrAc8** has an equilibrium concentration that could be measured (32 ± 6 mM), while no polymerization was observed when Grubbs third generation bis-pyridyl complex was added to neat **iPrAc7** or **iPrSi7**, suggesting that the equilibrium concentration for these two monomers is above their bulk concentration. In all cases, the model fit the data well, and the best fit parameters are listed in Table 1. Fitting these data using the Meyer-Lowry equation gave worse fits (as determined by the value of SSR, typically more than one order of magnitude larger, Table S3) and statistically significantly different values of reactivity ratios were obtained, highlighting the importance of using accurate models to fit data to discern specific trends. Interestingly, the best fit value of equilibrium concentration for **iPrSi7** is below its bulk concentration (1.5M versus ~5M), suggesting that bulk homopolymerization should be feasible from a thermodynamic perspective. This is in-line with our observations of no homopolymerization under modest solution conditions (1M) but contrasts with our observation of

no homopolymerization from the bulk. We posit then that absence of homopolymerization under bulk conditions for **iPrSi7** may be due to other effects, such as the possibility of a deleterious monomer isomerization-catalyst deactivation process.[63] Within this library of monomers, distinct copolymerization reactivity is observed based on the measured reactivity ratios: both **iPrSi8** and **iPrAc7** display strong alternating tendency as both reactivity ratios are < 1 (however, total **iPrAc7** incorporation is minimal), while **iPrSi7** copolymerizes with gradient behavior, and **iPrAc8** copolymerizes in a blocky fashion (both $r_{endo\text{-}NB}$, r_{iPrAc8} >1). We posit that such distinct reactivity behavior may explain differences in the efficacy for degradability in pDCPD copolymer systems with each of these cleavable comonomers.[83] Further correlation of cleavable comonomer structure and thermoset/plastic deconstruction behavior guided by these results are underway in our laboratories.

Table 1. Fit reactivity ratios and depropagation rate coefficients for the data presented in Figure 3. Uncertainties are determined through bootstrapping method and the bounds of 95% confidence intervals are listed in parentheses. For iPrSi8 and iPrAc8 the value of $\beta_{Comonomer}$ was independently measured and the uncertainty is presented as the result of a triplicate measurement.

Comonomer	$r_{endo\text{-}NB}$	$r_{Comonomer}$	$\beta_{Comonomer}$ [M]	$\gamma_{Comonomer}$ [M]
iPrSi8	0.40 (0.38, 0.49)	0.08 (0.03, 0.19)	0.047 (0.043, 0.051)	0.15 (0.09, 0.20)
iPrSi7	2.0 (1.9, 2.1)	0.01 (0.005, 0.015)	1.5 (1.3, 1.7)	0.13 (0.10, 0.15)
iPrAc8	1.5 (1.1, 1.6)	5.4 (4.1, 6.3)	0.032 (0.026, 0.038)	0.14 (0.10, 0.20)
iPrAc7	0.45 (0.035, 0.55)	0.7 (0.5, 1.1)	3.9 (3.4, 4.3)	4.2 (2.8, 5.7)

Next, we sought to characterize the ROMP copolymerization of dihydrofuran (**DHF**), a cyclic enol-ether, as an additional class of cleavable comonomer that has been applied to linear polymeric and thermoset materials.[66,86] Previously, one of our groups reported the use of dihydrofuran in copolymerizations with *exo*-norbornene monomers to yield acid-degradable polymers.[65] Fitting copolymerization data for such systems using the Meyer-Lowry equation yielded reactivity ratios of $r_{exo\text{-}NB} = 0.41$, $r_{DHF} = 0.088$, suggesting a strong alternating copolymerization behavior (i.e., $r_{exo-NB} \times r_{DHF} = 0.036 \ll 1$).[65] Interestingly, these reactivity ratio values contradict expected reactivity trends for ruthenium-based olefin metathesis catalysts, where electron-rich Ru Fischer

carbenes (as would exist for a DHF terminal chain end) are known to exhibit metathesis selectivity with similarly electron-rich olefins over electronically neutral olefins such as **exo-NB**, suggesting that the value of r_{DHF} should be significantly greater than 1.[87–89] We attribute this discrepancy to the fact that the copolymerization proceeded well below the equilibrium concentration of **DHF** (3.2 M), which was not captured in the Meyer-Lowry model and would lead to misinterpretation as alternating behavior due to the thermodynamic drive for DHF to propagate from a norbornene chain end but not subsequently homopolymerize below its equilibrium concentration.[86] We re-fit the previously reported ***exo*-NB** and **DHF** copolymerization data using the methods developed herein and obtained values of $r_{exo\text{-}NB} = 0.26$, $r_{DHF} = 5.3$, and $\gamma = 0.02$ M. Notably, the value of r_{DHF} is different by a factor of 60 compared to the Meyer-Lowry fitting and falls more in line with expectations for Grubbs-type ROMP initiators (i.e., r_{DHF} would be expected to be >1). Further the value of $\gamma \ll 1$ is consistent with the rate of depropagation of a DHF unit to reveal a norbornene chain end being relatively irreversible. Finally, we applied copolymer equation integration to re-evaluate the characterization of two previously reported copolymerization data sets for glycolide/lactide[46] and poly(ethylene glycol) methyl ether methacrylate ($PEGMA_9$) / 2-(diethylamino)ethyl methacrylate (DEAEMA)[32] where both comonomers are known to exhibit reversible propagation behavior.[90–92] In both cases, previous fitting had been conducted under the simplification that only one of the two comonomers could polymerize reversibly (lactide and $PEGMA_9$). In the case of glycolide/lactide, fitting data with a model that considers reversible propagation of *both* comonomers allowed us to distinguish between the effects of glycolide depropagation and transesterification reactions at high glycolide loadings. Additionally, in the case of $PEGMA_9$/DEAEMA, such a method provided significantly improved fits of the data and produced best fit parameters consistent with observations of incomplete comonomer consumption and measurements of comonomer equilibrium concentrations (see the Re-evaluation of Previously Reported Data Section of the Supporting Information for complete details). Altogether, these experimental examples highlight the importance of using suitable copolymerization models to characterize copolymerization reactivity to extract accurate and meaningful values of various rate coefficients and interpret experimental data.

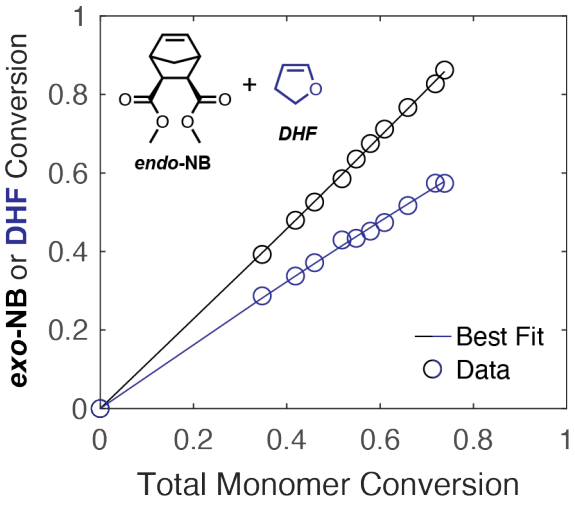

Figure 5. Copolymerization data and best fit for ***exo-NB*** and **DHF** reproduced from Ref. [65].

Conclusion

We have addressed a critical knowledge gap regarding the accurate characterization of reactivity ratios and other rate coefficients for two-component equilibrium copolymerization reactions. We present a detailed analysis of multiple methods to characterize this class of copolymerization reactions and demonstrate their general precision and accuracy. We rectify mistakes present in two original publications that derive equilibrium copolymer equations, assert the consistency between disparate forms of copolymer equations, and identify where the assumptions used in their derivations are invalidated. Additionally, a practical population balance method is introduced for these systems. We make recommendations for the process of data fitting and show that through transiently setting homopropagation rate coefficients equal to unity, the number of fit parameters can be reduced with no loss of accuracy and enables others to be measured independently of copolymerization experiments. It is shown that linearized methods and other simplified models previously used in the literature are inaccurate, and we discourage their further use. As proof-of-concept, we fit seven sets of equilibrium copolymerization data, giving chemically intuitive insights into copolymerization behaviors, and highlighting the utility of the methods evaluated herein. The analysis and tools presented in this work will enable the rapid, simple, and accurate evaluation of equilibrium copolymerization reactions toward the development of chemically recyclable polymers, circular materials, and advanced data-driven methods and predictions.

Acknowledgements. This work was supported as part of the Center for Regenerative Energy-Efficient Manufacturing of Thermoset Polymeric Materials (REMAT), an Energy Frontier Research Center funded by the U.S. Department of Energy, Office of Science, Basic Energy Sciences under award #DE-SC0023457.

References.

(1) *Modern Styrenic Polymers: Polystyrenes and Styrenic Copolymers*; Scheirs, J., Priddy, D. B., Eds.; Wiley, 2003. https://doi.org/10.1002/0470867213.

(2) Raval, N.; Kalyane, D.; Maheshwari, R.; Tekade, R. K. Copolymers and Block Copolymers in Drug Delivery and Therapy. In *Basic Fundamentals of Drug Delivery*; Elsevier, 2019; pp 173–201. https://doi.org/10.1016/B978-0-12-817909-3.00005-4.

(3) Mayo, F. R.; Walling, Cheves. Copolymerization. *Chem Rev* **1950**, *46* (2), 191–287. https://doi.org/10.1021/cr60144a001.

(4) Yasir, M.; Liu, P.; Markwart, J. C.; Suraeva, O.; Wurm, F. R.; Smart, J.; Lattuada, M.; Kilbinger, A. F. M. One-Step Ring Opening Metathesis Block-Like Copolymers and Their Compositional Analysis by a Novel Retardation Technique. *Angewandte Chemie International Edition* **2020**, *59* (32), 13597–13601. https://doi.org/10.1002/anie.202005366.

(5) Kenney, J. F. Properties of Block versus Random Copolymers. *Polym Eng Sci* **1968**, *8* (3), 216–226. https://doi.org/10.1002/pen.760080307.

(6) Lin, T.-P.; Chang, A. B.; Chen, H.-Y.; Liberman-Martin, A. L.; Bates, C. M.; Voegtle, M. J.; Bauer, C. A.; Grubbs, R. H. Control of Grafting Density and Distribution in Graft Polymers by Living Ring-Opening Metathesis Copolymerization. *J Am Chem Soc* **2017**, *139* (10), 3896–3903. https://doi.org/10.1021/jacs.7b00791.

(7) Mayo, F. R.; Lewis, F. M. Copolymerization. I. A Basis for Comparing the Behavior of Monomers in Copolymerization; The Copolymerization of Styrene and Methyl Methacrylate. *J Am Chem Soc* **1944**, *66* (9), 1594–1601. https://doi.org/10.1021/ja01237a052.

(8) Fineman, M.; Ross, S. D. Linear Method for Determining Monomer Reactivity Ratios in Copolymerization. *Journal of Polymer Science* **1950**, *5* (2), 259–262. https://doi.org/10.1002/pol.1950.120050210.

(9) Kennedy, J. P.; Kelen, T.; Tüdös, F. Analysis of the Linear Methods for Determining Copolymerization Reactivity Ratios. II. A Critical Reexamination of Cationic Monomer Reactivity Ratios. *Journal of Polymer Science: Polymer Chemistry Edition* **1975**, *13* (10), 2277–2289. https://doi.org/10.1002/pol.1975.170131010.

(10) O'Driscoll, K. F.; Reilly, P. M. Determination of Reactivity Ratios in Copolymerization. *Makromolekulare Chemie. Macromolecular Symposia* **1987**, *10–11* (1), 355–374. https://doi.org/10.1002/masy.19870100118.

(11) Kazemi, N.; Duever, T. A.; Penlidis, A. Reactivity Ratio Estimation from Cumulative Copolymer Composition Data. *Macromol React Eng* **2011**, *5* (9–10), 385–403. https://doi.org/10.1002/mren.201100009.

(12) Lynd, N. A.; Ferrier, R. C.; Beckingham, B. S. Recommendation for Accurate Experimental Determination of Reactivity Ratios in Chain Copolymerization.

Macromolecules **2019**, *52* (6), 2277–2285. https://doi.org/10.1021/acs.macromol.8b01752.
(13) McFarlane, R. C.; Reilly, P. M.; O'driscoll, K. F. Comparison of the Precision of Estimation of Copolymerization Reactivity Ratios by Current Methods. *Journal of Polymer Science: Polymer Chemistry Edition* **1980**, *18* (1), 251–257. https://doi.org/10.1002/pol.1980.170180123.
(14) Shawki, S. M.; Hamielec, A. E. Estimation of the Reactivity Ratios in the Copolymerization of Acrylic Acid and Acrylamide from Composition–Conversion Measurements by an Improved Nonlinear Least-Squares Method. *J Appl Polym Sci* **1979**, *23* (11), 3155–3166. https://doi.org/10.1002/app.1979.070231102.
(15) Fierens, S. K.; Van Steenberge, P. H. M.; Reyniers, M.-F.; D'hooge, D. R.; Marin, G. B. Analytical and Advanced Kinetic Models for Characterization of Chain-Growth Copolymerization: The State-of-the-Art. *React Chem Eng* **2018**, *3* (2), 128–145. https://doi.org/10.1039/C7RE00206H.
(16) Meyer, V. E.; Lowry, G. G. Integral and Differential Binary Copolymerization Equations. *J Polym Sci A* **1965**, *3* (8), 2843–2851. https://doi.org/10.1002/pol.1965.100030811.
(17) Smith, A. A. A.; Hall, A.; Wu, V.; Xu, T. Practical Prediction of Heteropolymer Composition and Drift. *ACS Macro Lett* **2019**, *8* (1), 36–40. https://doi.org/10.1021/acsmacrolett.8b00813.
(18) Sawada, H. Thermodynamics of Polymerization. I. *Journal of Macromolecular Science, Part C: Polymer Reviews* **1969**, *3* (2), 313–338. https://doi.org/10.1080/15583726908545926.
(19) Warfield, R. W.; Petree, M. C. Thermodynamic Properties of Polystyrene and Styrene. *Journal of Polymer Science* **1961**, *55* (162), 497–505. https://doi.org/10.1002/pol.1961.1205516208.
(20) Lowry, G. G. The Effect of Depropagation on Copolymer Composition. I. General Theory for One Depropagating Monomer. *Journal of Polymer Science* **1960**, *42* (140), 463–477. https://doi.org/10.1002/pol.1960.1204214014.
(21) Yee, L. H.; Heuts, J. P. A.; Davis, T. P. Copolymerization Propagation Kinetics of Dimethyl Itaconate and Styrene: Strong Entropic Contributions to the Penultimate Unit Effect. *Macromolecules* **2001**, *34* (11), 3581–3586. https://doi.org/10.1021/ma001952s.
(22) Fukuda, T.; Ma, Y. D.; Inagaki, H.; Kubo, K. Penultimate-Unit Effects in Free-Radical Copolymerization. *Macromolecules* **1991**, *24* (2), 370–375. https://doi.org/10.1021/ma00002a005.
(23) Hill, D. J. T.; Lang, A. P.; O'Donnell, J. H.; O'Sullivan, P. W. Determination of Reactivity Ratios from Analysis of Triad Fractions—Analysis of the Copolymerization of Styrene and Acrylonitrile as Evidence for the Penultimate Model. *Eur Polym J* **1989**, *25* (9), 911–915. https://doi.org/10.1016/0014-3057(89)90109-2.
(24) Barson, C. A.; Fenn, D. R. A Method for Determining Reactivity Ratios When Copolymerizations Are Influenced by the Penultimate Group Effects of Both Monomers. *Eur Polym J* **1989**, *25* (7–8), 719–720. https://doi.org/10.1016/0014-3057(89)90035-9.
(25) KAIM, A. Terminal and Penultimate Reactivity Ratios in the Styrene-Acrylonitrile Free-Radical Copolymerization System in Bulk. *Journal of Macromolecular Science, Part A* **1998**, *35* (4), 577–588. https://doi.org/10.1080/10601329808001998.
(26) Ono, K.; Teramachi, S. Penultimate Unit Effects in Free-Radical Copolymerization. Number-Average Degree of Polymerization and Copolymerization Rate in Styrene/Methyl

Methacrylate/Toluene System. *Polym J* **1995**, *27* (8), 790–796. https://doi.org/10.1295/polymj.27.790.
(27) Deb, P. C. Determination of Penultimate Model Reactivity Ratios and Their Non-Uniqueness. *Polymer (Guildf)* **2007**, *48* (2), 432–436. https://doi.org/10.1016/j.polymer.2006.11.027.
(28) O'Driscoll, K. F.; Reilly, P. M. Determination of Reactivity Ratios in Copolymerization. *Makromolekulare Chemie. Macromolecular Symposia* **1987**, *10–11* (1), 355–374. https://doi.org/10.1002/masy.19870100118.
(29) Hazell, J. E.; Ivin, K. J. Copolymerization of Pairs of Olefines with Sulphur Dioxide in the Region of the Ceiling Temperature. *Transactions of the Faraday Society* **1962**, *58*, 342. https://doi.org/10.1039/tf9625800342.
(30) O'driscoll, K. F.; Gasparro, F. P. Copolymerization with Depropagation. *Journal of Macromolecular Science: Part A - Chemistry* **1967**, *1* (4), 643–652. https://doi.org/10.1080/10601326708054001.
(31) Harrisson, S.; Davis, T. P.; Evans, R. A.; Rizzardo, E. Copolymerization Behavior of 7-Methylene-2-Methyl-1,5-Dithiacyclooctane: Reversible Cross-Propagation. *Macromolecules* **2001**, *34* (12), 3869–3876. https://doi.org/10.1021/ma0020584.
(32) Cabello-Romero, J.; Torres-Lubián, R.; Enríquez-Medrano, F. J.; Hutchinson, R. A.; Zapata-González, I. The Influence of Depropagation on PEGMA $_9$ Solution Radical Homopolymerization and Copolymerization with DEAEMA: *In Situ* ^{1} H-NMR Measurements and Reactivity Ratio Estimation by Dynamic Optimization. *Polym Chem* **2024**. https://doi.org/10.1039/D3PY01087B.
(33) WITTMER, P. Copolymerization in the Presence of Depolymerization Reactions; 1971; pp 140–174. https://doi.org/10.1021/ba-1971-0099.ch010.
(34) Ito, K.; Kodaira, K. Kinetics of Radical Copolymerization between α-Methylstyrene and Methyl Methacrylate. *Polym J* **1986**, *18* (9), 667–672. https://doi.org/10.1295/polymj.18.667.
(35) Albanese, K. R.; Okayama, Y.; Morris, P. T.; Gerst, M.; Gupta, R.; Speros, J. C.; Hawker, C. J.; Choi, C.; de Alaniz, J. R.; Bates, C. M. Building Tunable Degradation into High-Performance Poly(Acrylate) Pressure-Sensitive Adhesives. *ACS Macro Lett* **2023**, *12* (6), 787–793. https://doi.org/10.1021/acsmacrolett.3c00204.
(36) Palmer, D. E.; McManus, N. T.; Penlidis, A. Copolymerization with Depropagation: A Study of ?-Methyl Styrene/Methyl Methacrylate in Bulk at Elevated Temperatures. *J Polym Sci A Polym Chem* **2000**, *38* (11), 1981–1990. https://doi.org/10.1002/(SICI)1099-0518(20000601)38:11<1981::AID-POLA70>3.0.CO;2-6.
(37) Palmer, D. E.; McManus, N. T.; Penlidis, A. Copolymerization with Depropagation: A Study of A-methyl Styrene/Methyl Methacrylate in Solution at Elevated Temperatures. *J Polym Sci A Polym Chem* **2001**, *39* (10), 1753–1763. https://doi.org/10.1002/pola.1153.
(38) Howell, J. A.; Izu, M.; O'Driscoll, K. F. Copolymerization with Depropagation. III. Composition and Sequence Distribution from Probability Considerations. *J Polym Sci A1* **1970**, *8* (3), 699–710. https://doi.org/10.1002/pol.1970.150080313.
(39) Krüger, H.; Bauer, J.; Rübner, J. Ein Modell Zur Beschreibung Reversibler Copolymerisationen. *Die Makromolekulare Chemie* **1987**, *188* (9), 2163–2175. https://doi.org/10.1002/macp.1987.021880913.

(40) McManus, N. T.; Penlidis, A.; Dube, M. A. Copolymerization of Alpha-Methyl Styrene with Butyl Acrylate in Bulk. *Polymer (Guildf)* **2002**, *43* (5), 1607–1614. https://doi.org/10.1016/S0032-3861(01)00738-8.
(41) Wang, T. J.; Leamen, M. J.; McManus, N. T.; Penlidis, A. Copolymerization of Alpha-Methyl Styrene with Butyl Acrylate: Parameter Estimation Considerations. *Journal of Macromolecular Science, Part A* **2004**, *41* (11), 1205–1220. https://doi.org/10.1081/MA-200029827.
(42) Leamen, M. J.; McManus, N. T.; Penlidis, A. Binary Copolymerization with Full Depropagation: A Study of Methyl Methacrylate/A-methyl Styrene Copolymerization. *J Polym Sci A Polym Chem* **2005**, *43* (17), 3868–3877. https://doi.org/10.1002/pola.20874.
(43) Szymański, R. Reversible Copolymerization at Equilibrium. *Die Makromolekulare Chemie* **1986**, *187* (5), 1109–1114. https://doi.org/10.1002/macp.1986.021870507.
(44) Szymanski, R. Thermodynamics of Copolymerization. *Prog Polym Sci* **1992**, *17* (5), 917–951. https://doi.org/10.1016/0079-6700(92)90013-O.
(45) Torre, M.; Mulhearn, W. D.; Register, R. A. Ring-Opening Metathesis Copolymerization of Cyclopentene Above and Below Its Equilibrium Monomer Concentration. *Macromol Chem Phys* **2018**, *219* (9), 1800030. https://doi.org/10.1002/macp.201800030.
(46) Kuehster, L.; Jhon, Y. K.; Wang, Y.; Smith, W. C.; Xu, X.; Qin, B.; Zhang, F.; Lynd, N. A. Stochastic and Deterministic Analysis of Reactivity Ratios in the Partially Reversible Copolymerization of Lactide and Glycolide. *Macromolecules* **2022**, *55* (16), 7171–7180. https://doi.org/10.1021/acs.macromol.2c00757.
(47) Lodge, T. P.; Hiemenz, P. C. *Polymer Chemistry*; CRC Press: Third edition. | Boca Raton : CRC Press, 2020., 2020. https://doi.org/10.1201/9780429190810.
(48) Odian, G. *Principles of Polymerization*; Wiley, 2004. https://doi.org/10.1002/047147875X.
(49) Kaitz, J. A.; Moore, J. S. Functional Phthalaldehyde Polymers by Copolymerization with Substituted Benzaldehydes. *Macromolecules* **2013**, *46* (3), 608–612. https://doi.org/10.1021/ma302575s.
(50) Engler, A.; Phillips, O.; Miller, R. C.; Tobin, C.; Kohl, P. A. Cationic Copolymerization of *o* -Phthalaldehyde and Functional Aliphatic Aldehydes. *Macromolecules* **2019**, *52* (11), 4020–4029. https://doi.org/10.1021/acs.macromol.9b00740.
(51) Čamdžić, L.; Stache, E. E. Controlled Radical Polymerization of Acrylates and Isocyanides Installs Degradable Functionality into Novel Copolymers. *J Am Chem Soc* **2023**, *145* (37), 20311–20318. https://doi.org/10.1021/jacs.3c04595.
(52) Nasresfahani, A.; Idowu, L. A.; Hutchinson, R. A. Extractable Content of Functional Acrylic Resins Produced by Radical Copolymerization: A Comparison of Experiment and Stochastic Simulation. *Chemical Engineering Journal* **2019**, *378*, 122087. https://doi.org/10.1016/j.cej.2019.122087.
(53) Coates, G. W.; Getzler, Y. D. Y. L. Chemical Recycling to Monomer for an Ideal, Circular Polymer Economy. *Nat Rev Mater* **2020**, *5* (7), 501–516. https://doi.org/10.1038/s41578-020-0190-4.
(54) Jones, G. R.; Wang, H. S.; Parkatzidis, K.; Whitfield, R.; Truong, N. P.; Anastasaki, A. Reversed Controlled Polymerization (RCP): Depolymerization from Well-Defined Polymers to Monomers. *J Am Chem Soc* **2023**, *145* (18), 9898–9915. https://doi.org/10.1021/jacs.3c00589.

(55) Deng, Z.; Gillies, E. R. Emerging Trends in the Chemistry of End-to-End Depolymerization. *JACS Au* **2023**, *3* (9), 2436–2450. https://doi.org/10.1021/jacsau.3c00345.
(56) Young, J. B.; Hughes, R. W.; Tamura, A. M.; Bailey, L. S.; Stewart, K. A.; Sumerlin, B. S. Bulk Depolymerization of Poly(Methyl Methacrylate) via Chain-End Initiation for Catalyst-Free Reversion to Monomer. *Chem* **2023**, *9* (9), 2669–2682. https://doi.org/10.1016/j.chempr.2023.07.004.
(57) Li, S.; Pignol, M.; Gasc, F.; Vert, M. Synthesis, Characterization, and Enzymatic Degradation of Copolymers Prepared from ε-Caprolactone and β-Butyrolactone. *Macromolecules* **2004**, *37* (26), 9798–9803. https://doi.org/10.1021/ma0489422.
(58) Takebayashi, K.; Kanazawa, A.; Aoshima, S. Cationic Ring-Opening Copolymerization of a Cyclic Acetal and γ-Butyrolactone: Monomer Sequence Transformation and Polymerization–Depolymerization Control by Vacuuming or Temperature Changes. *Polym J* **2023**. https://doi.org/10.1038/s41428-023-00847-9.
(59) Gilsdorf, R. A.; Nicki, M. A.; Chen, E. Y.-X. High Chemical Recyclability of Vinyl Lactone Acrylic Bioplastics. *Polym Chem* **2020**, *11* (30), 4942–4950. https://doi.org/10.1039/D0PY00786B.
(60) Christoff-Tempesta, T.; O'Dea, R. M.; Epps, T. H. Unlocking Circularity Through the Chemical Recycling and Upcycling of Lignin-Derivable Polymethacrylates. *Macromolecules* **2023**, *56* (23), 9796–9803. https://doi.org/10.1021/acs.macromol.3c01985.
(61) Holmberg, A. L.; Reno, K. H.; Nguyen, N. A.; Wool, R. P.; Epps, T. H. Syringyl Methacrylate, a Hardwood Lignin-Based Monomer for High- T_g Polymeric Materials. *ACS Macro Lett* **2016**, *5* (5), 574–578. https://doi.org/10.1021/acsmacrolett.6b00270.
(62) Shieh, P.; Nguyen, H. V.-T.; Johnson, J. A. Tailored Silyl Ether Monomers Enable Backbone-Degradable Polynorbornene-Based Linear, Bottlebrush and Star Copolymers through ROMP. *Nat Chem* **2019**, *11* (12), 1124–1132. https://doi.org/10.1038/s41557-019-0352-4.
(63) Johnson, A. M.; Husted, K. E. L.; Kilgallon, L. J.; Johnson, J. A. Orthogonally Deconstructable and Depolymerizable Polysilylethers *via* Entropy-Driven Ring-Opening Metathesis Polymerization. *Chemical Communications* **2022**, *58* (61), 8496–8499. https://doi.org/10.1039/D2CC02718F.
(64) Shieh, P.; Zhang, W.; Husted, K. E. L.; Kristufek, S. L.; Xiong, B.; Lundberg, D. J.; Lem, J.; Veysset, D.; Sun, Y.; Nelson, K. A.; Plata, D. L.; Johnson, J. A. Cleavable Comonomers Enable Degradable, Recyclable Thermoset Plastics. *Nature* **2020**, *583* (7817), 542–547. https://doi.org/10.1038/s41586-020-2495-2.
(65) Feist, J. D.; Lee, D. C.; Xia, Y. A Versatile Approach for the Synthesis of Degradable Polymers via Controlled Ring-Opening Metathesis Copolymerization. *Nat Chem* **2022**, *14* (1), 53–58. https://doi.org/10.1038/s41557-021-00810-2.
(66) Davydovich, O.; Paul, J. E.; Feist, J. D.; Aw, J. E.; Balta Bonner, F. J.; Lessard, J. J.; Tawfick, S.; Xia, Y.; Sottos, N. R.; Moore, J. S. Frontal Polymerization of Dihydrofuran Comonomer Facilitates Thermoset Deconstruction. *Chemistry of Materials* **2022**, *34* (19), 8790–8797. https://doi.org/10.1021/acs.chemmater.2c02045.
(67) Albanese, K. R.; Morris, P. T.; Read de Alaniz, J.; Bates, C. M.; Hawker, C. J. Controlled-Radical Polymerization of α-Lipoic Acid: A General Route to Degradable Vinyl

Copolymers. *J Am Chem Soc* **2023**, *145* (41), 22728–22734. https://doi.org/10.1021/jacs.3c08248.
(68) Watanabe, H.; Kamigaito, M. Direct Radical Copolymerizations of Thioamides To Generate Vinyl Polymers with Degradable Thioether Bonds in the Backbones. *J Am Chem Soc* **2023**, *145* (20), 10948–10953. https://doi.org/10.1021/jacs.3c01796.
(69) Martin, T. B.; Audus, D. J. Emerging Trends in Machine Learning: A Polymer Perspective. *ACS Polymers Au* **2023**, *3* (3), 239–258. https://doi.org/10.1021/acspolymersau.2c00053.
(70) Nguyen, T.; Bavarian, M. Machine Learning Approach to Polymer Reaction Engineering: Determining Monomers Reactivity Ratios. *Polymer (Guildf)* **2023**, *275*, 125866. https://doi.org/10.1016/j.polymer.2023.125866.
(71) Walsh, D. J.; Zou, W.; Schneider, L.; Mello, R.; Deagen, M. E.; Mysona, J.; Lin, T.-S.; de Pablo, J. J.; Jensen, K. F.; Audus, D. J.; Olsen, B. D. Community Resource for Innovation in Polymer Technology (CRIPT): A Scalable Polymer Material Data Structure. *ACS Cent Sci* **2023**, *9* (3), 330–338. https://doi.org/10.1021/acscentsci.3c00011.
(72) AlFaraj, Y. S.; Mohapatra, S.; Shieh, P.; Husted, K. E. L.; Ivanoff, D. G.; Lloyd, E. M.; Cooper, J. C.; Dai, Y.; Singhal, A. P.; Moore, J. S.; Sottos, N. R.; Gomez-Bombarelli, R.; Johnson, J. A. A Model Ensemble Approach Enables Data-Driven Property Prediction for Chemically Deconstructable Thermosets in the Low-Data Regime. *ACS Cent Sci* **2023**, *9* (9), 1810–1819. https://doi.org/10.1021/acscentsci.3c00502.
(73) Szymanski, R.; Sosnowski, S.; Cypryk, M. Evolution of Chain Microstructure and Kinetics of Reaching Equilibrium in Living Reversible Copolymerization. *Macromol Theory Simul* **2016**, *25* (2), 196–214. https://doi.org/10.1002/mats.201500047.
(74) Ali Parsa, M.; Kozhan, I.; Wulkow, M.; Hutchinson, R. A. Modeling of Functional Group Distribution in Copolymerization: A Comparison of Deterministic and Stochastic Approaches. *Macromol Theory Simul* **2014**, *23* (3), 207–217. https://doi.org/10.1002/mats.201300156.
(75) Rego, A. S. C.; Brandão, A. L. T. General Method for Speeding Up Kinetic Monte Carlo Simulations. *Ind Eng Chem Res* **2020**, *59* (19), 9034–9042. https://doi.org/10.1021/acs.iecr.0c01069.
(76) Wang, W.; Hutchinson, R. A. A Comprehensive Kinetic Model for High-temperature Free Radical Production of Styrene/Methacrylate/Acrylate Resins. *AIChE Journal* **2011**, *57* (1), 227–238. https://doi.org/10.1002/aic.12258.
(77) Schier, J. E. S.; Zhang, M.; Grady, M. C.; Hutchinson, R. A. Modeling of Semibatch Solution Radical Copolymerization of Butyl Methacrylate and 2-Hydroxyethyl Acrylate. *Macromol React Eng* **2018**, *12* (4). https://doi.org/10.1002/mren.201800008.
(78) Dorschner, D.; Jung, W.; Riahinezhad, M.; Duever, T. A.; Penlidis, A. Case Studies with Mathematical Modeling of Free-Radical Multi-Component Bulk/Solution Polymerizations: Part 2. *Journal of Macromolecular Science, Part A* **2017**, *54* (6), 339–371. https://doi.org/10.1080/10601325.2017.1312678.
(79) Jung, W.; Riahinezhad, M.; Duever, T. A.; Penlidis, A. Case Studies With Mathematical Modeling of Free-Radical Multi-Component Bulk/Solution Polymerizations: Part 1. *Journal of Macromolecular Science, Part A* **2015**, *52* (9), 659–698. https://doi.org/10.1080/10601325.2015.1063861.

(80) Olsén, P.; Odelius, K.; Albertsson, A.-C. Thermodynamic Presynthetic Considerations for Ring-Opening Polymerization. *Biomacromolecules* **2016**, *17* (3), 699–709. https://doi.org/10.1021/acs.biomac.5b01698.
(81) Hlil, A. R.; Balogh, J.; Moncho, S.; Su, H.-L.; Tuba, R.; Brothers, E. N.; Al-Hashimi, M.; Bazzi, H. S. Ring Opening Metathesis Polymerization (ROMP) of Five- to Eight-Membered Cyclic Olefins: Computational, Thermodynamic, and Experimental Approach. *J Polym Sci A Polym Chem* **2017**, *55* (18), 3137–3145. https://doi.org/10.1002/pola.28695.
(82) Greer, S. C. Physical Chemistry of Equilibrium Polymerization. *J Phys Chem B* **1998**, *102* (28), 5413–5422. https://doi.org/10.1021/jp981592z.
(83) Lloyd, E. M.; Cooper, J. C.; Shieh, P.; Ivanoff, D. G.; Parikh, N. A.; Mejia, E. B.; Husted, K. E. L.; Costa, L. C.; Sottos, N. R.; Johnson, J. A.; Moore, J. S. Efficient Manufacture, Deconstruction, and Upcycling of High-Performance Thermosets and Composites. *ACS Applied Engineering Materials* **2023**, *1* (1), 477–485. https://doi.org/10.1021/acsaenm.2c00115.
(84) Shieh, P.; Hill, M. R.; Zhang, W.; Kristufek, S. L.; Johnson, J. A. Clip Chemistry: Diverse (Bio)(Macro)Molecular and Material Function through Breaking Covalent Bonds. *Chem Rev* **2021**, *121* (12), 7059–7121. https://doi.org/10.1021/acs.chemrev.0c01282.
(85) Kirkland, T. A.; Grubbs, R. H. Effects of Olefin Substitution on the Ring-Closing Metathesis of Dienes. *J Org Chem* **1997**, *62* (21), 7310–7318. https://doi.org/10.1021/jo970877p.
(86) Feist, J. D.; Xia, Y. Enol Ethers Are Effective Monomers for Ring-Opening Metathesis Polymerization: Synthesis of Degradable and Depolymerizable Poly(2,3-Dihydrofuran). *J Am Chem Soc* **2020**, *142* (3), 1186–1189. https://doi.org/10.1021/jacs.9b11834.
(87) Louie, J.; Grubbs, R. H. Metathesis of Electron-Rich Olefins: Structure and Reactivity of Electron-Rich Carbene Complexes. *Organometallics* **2002**, *21* (11), 2153–2164. https://doi.org/10.1021/om011037a.
(88) Katayama, H.; Urushima, H.; Nishioka, T.; Wada, C.; Nagao, M.; Ozawa, F. Highly Selective Ring-Opening/Cross-Metathesis Reactions of Norbornene Derivatives Using Selenocarbene Complexes as Catalysts. *Angewandte Chemie International Edition* **2000**, *39* (24), 4513–4515. https://doi.org/10.1002/1521-3773(20001215)39:24<4513::AID-ANIE4513>3.0.CO;2-C.
(89) Katayama, H.; Yonezawa, F.; Nagao, M.; Ozawa, F. Ring-Opening Metathesis Polymerization of Norbornene Using Vinylic Ethers as Chain-Transfer Agents: Highly Selective Synthesis of Monofunctional Macroinitiators for Atom Transfer Radical Polymerization. *Macromolecules* **2002**, *35* (3), 1133–1136. https://doi.org/10.1021/ma0110249.
(90) Sedush, N. G.; Strelkov, Yu. Yu.; Chvalun, S. N. Kinetic Investigation of the Polymerization of D,L-Lactide and Glycolide via Differential Scanning Calorimetry. *Polymer Science Series B* **2014**, *56* (1), 35–40. https://doi.org/10.1134/S1560090414010102.
(91) Wang, Y.; Hillmyer, M. A. Synthesis of Polybutadiene−Polylactide Diblock Copolymers Using Aluminum Alkoxide Macroinitiators. Kinetics and Mechanism. *Macromolecules* **2000**, *33* (20), 7395–7403. https://doi.org/10.1021/ma0007177.
(92) Wang, H. S.; Truong, N. P.; Pei, Z.; Coote, M. L.; Anastasaki, A. Reversing RAFT Polymerization: Near-Quantitative Monomer Generation Via a Catalyst-Free

Depolymerization Approach. *J Am Chem Soc* **2022**, *144* (10), 4678–4684. https://doi.org/10.1021/jacs.2c00963.